

---

# Deep learning of normal form autoencoders for universal, parameter-dependent dynamics

---

**Manu Kalia**

Department of Applied Mathematics  
University of Twente  
m.kalia@utwente.nl

**Steven L. Brunton**

Department of Mechanical Engineering  
University of Washington

**Hil G.E. Meijer**

Department of Applied Mathematics  
University of Twente

**Christoph Brune**

Department of Applied Mathematics  
University of Twente

**J. Nathan Kutz**

Department of Applied Mathematics  
University of Washington

## Abstract

A long-standing goal in dynamical systems is to construct reduced-order models for high-dimensional spatiotemporal data that capture the underlying parametric dependence of the data. In this work, we introduce a deep learning technique to discover a single low-dimensional model for such data that captures the underlying parametric dependence in terms of a *normal form*. A normal form is a symbolic expression, or universal unfolding, that describes how a the reduced-order differential equation model varies with respect to a bifurcation parameter. Our approach introduces coupled autoencoders for the state and parameter, with the latent variables constrained to adhere to a given normal form. We demonstrate our method on one-parameter bifurcations that occur in the canonical Lorenz96 equations and a neural field equation. This method demonstrates how normal forms can be leveraged as canonical and universal building blocks in deep learning approaches for model discovery and reduced-order modeling.

## 1 Introduction

Discovery of reduced-order models from high-dimensional spatiotemporal data is central to a qualitative understanding of underlying characteristics in dynamics [1, 2]. Current approaches include modal decomposition techniques, such as proper orthogonal decomposition (POD) and dynamic mode decomposition (DMD), which approximate low-dimensional projections by using linear maps between snapshots in time [3, 4, 5, 6, 7, 8, 9]. These methods are reinforced by model discovery techniques, such as sparse identification of nonlinear dynamics (SINDy), which can uncover parsimonious nonlinear models from data [10, 11]. However, the techniques above depend on a predefined candidate library of basis functions. Recent work has focused on combining model discovery and reduced-order modeling methods with neural networks and deep learning to remove this dependency [12, 13, 14, 15, 16, 17, 18, 19, 20, 21, 22, 23, 24, 25].

These methods, however, do not directly deal with temporal datasets originating from a single physical system across different experimental conditions and parametrizations. Such data can exhibit *topological inequivalence* [26], where two time-traces from the data cannot be mapped onto each

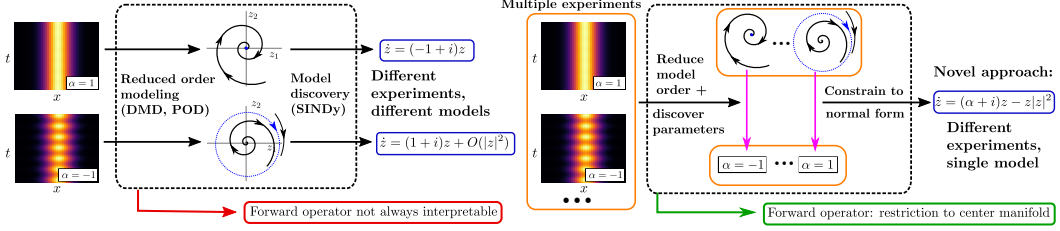


Figure 1: Overview of the state-of-the-art in the reduced-order modeling of parametric systems (left), resulting in isolated models for each parameter value. Our novel approach (right), uncovers a single parameterized equation (i.e., a normal form) that captures the parametric dependence across the data.

other by continuous invertible transformations. This presents a challenge for the aforementioned methods, as observations from a single physical system might yield irreconcilably different low-dimensional models. In this work, we present a first deep learning approach that extracts a single low-dimensional model, and its parametric dependence, from high dimensional temporal data of a single physical system across different experimental conditions.

A summary is presented in Fig. 1. The resulting low-dimensional models are *normal form equations*, which describe universal behaviour of transitions in topological equivalence (called *bifurcations*) [1, 26]. We do so by using neural networks that transform observations of states and parameters simultaneously while constraining the transformed variables to normal form equations. In this work, we focus on observations corresponding to a single bifurcation only. Moreover, the resulting transformation can be interpreted as a restriction of high-dimensional dynamics to the underlying low-dimensional theoretical *center manifold*, on which the interesting transitions occur.

## 2 Methods

Figure 2 describes the neural network architecture, the loss functions and the normal forms we consider. The architecture is composed of two fully connected adjoint autoencoders ( $\Phi_1, \varphi_1$ ) and ( $\Phi_2, \varphi_2$ ). They encode state  $x$  and parameter  $\alpha$  to the respective latent state  $z$  and parameter  $\beta$  such that  $\dot{x} = f(x, \alpha)$ , and  $\dot{z} = g(z, \beta)$  is a normal form equation. The architecture is inspired from [19] where we now add an extra autoencoder for the parameters  $\alpha$ . The various normal forms, with their equations and representative phase portraits are also presented in Fig. 2.

**Loss function:** We also show the loss function, that is composed of three kinds of terms. The ‘decoder loss’ refers to the two autoencoder loss terms. The ‘consistency loss’ couples the two autoencoders by constraining the latent variables  $z$  and  $\beta$  to the normal form equation  $\dot{z} = g(z, \beta)$ . Inductive biases are introduced in the ‘orientation loss’ that is composed of two terms, the zero-loss ( $\lambda_5 \|\Phi_1(0)\|_1$ ) and the parameter-orientation loss. We motivate these terms here.

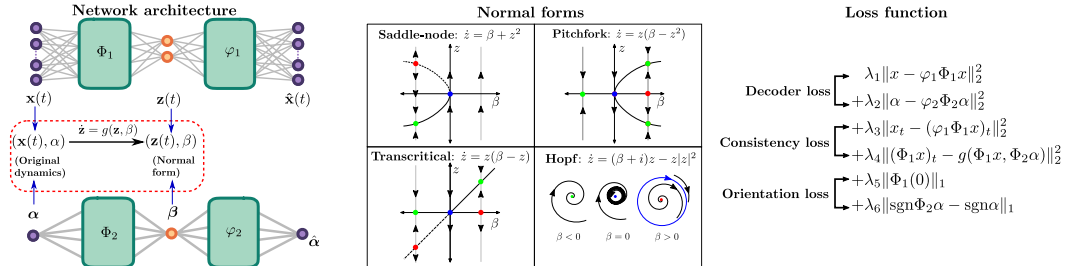


Figure 2: Summary of the method. We show the network architecture, the various normal forms considered in this work, and the loss function we use to constrain the data to the normal form. Throughout the work, we set  $\lambda_1 = \lambda_2 = \lambda_5 = \lambda_6 = 1$ , and  $\lambda_3 = \lambda_4 = 10^{-3}$ .

**Existence and uniqueness:** First, we note that the theory of normal forms and bifurcations guarantee a solution for the neural network parameters  $\Phi_i, \varphi_i$ . For any high-dimensional system undergoing

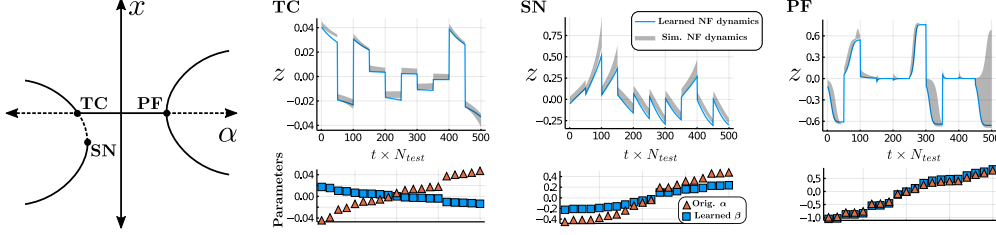


Figure 3: Results for the 1D system Eq. 1. For each bifurcation, 10 test traces are concatenated and presented. In all cases, training and test data contain 500 and 20 traces, respectively. The gray area shows an ensemble of 50 simulated trajectories.  $\Phi_1$  and  $\varphi_1$  have widths  $[20, 20]$  and  $[10, 10]$ .

a bifurcation, there exists a smooth transformation to a low-dimensional center manifold such that the dynamics on this manifold are described by the normal form equations [1, 26]. In our case, the transformation is smooth as we always use *elu* activation functions. Moreover, as a byproduct the autoencoder determines the center manifold. In classical literature on obtaining normal form equations [26], the center manifold is explicitly constructed which is only feasible for low-dimensional models. In order to use center manifold theory, the bifurcation in the original system  $\dot{x} = f(x, \alpha)$  is always shifted to  $(x, \alpha) = (0, 0)$ . In our training and test data we ensure this by appropriately translating the dataset. However, the center manifold is not unique. Thus, there may exist multiple solutions  $\Phi_i, \varphi_i$ .

**Inductive bias:** In order to deal with non-uniqueness and underlying local minima, we introduce the zero loss and the parameter-orientation loss. The zero loss forces the autoencoder to recognize that a zero solution in the original dynamics must correspond to a zero solution in the latent dynamics. This is necessary to make sure that we take into account the existence of the trivial solution in the normal form equation as an equilibrium in most cases. The parameter orientation loss fixes the direction of the bifurcation for the latent dynamics, by making sure that  $\alpha$  and  $\beta$  have the same sign, thereby eliminating several local minima.

**Training:** Initial conditions and parameters are chosen from a uniform distribution. They are shuffled and paired together, and then used together to simulate time traces, that form test and training data. Training is performed for 200 epochs with batch size 100 or till the test loss stabilizes, which is to  $\approx 1 \times 10^{-2}$  in all examples.

### 3 Results

In this section we present the use of our approach on a few examples, showcasing the most important local codimension one bifurcations: saddle-node, transcritical, pitchfork and Hopf.

**1D system with several bifurcations.** We start by looking at the following scalar ODE that contains multiple bifurcations,

$$\dot{x} = \gamma x(\alpha - \alpha_{pf} - x^2)(\alpha - \alpha_{sn} + (x - x_{sn})^2), \quad (1)$$

where we set  $\gamma = 0.01$ ,  $x_{sn} = \alpha_{sn} = -6$  and  $\alpha_{pf} = 6$ . Fig. 3 shows the bifurcation diagram for Eq. (1). The system exhibits saddle-node (at  $(x, \alpha) = (-6, -6)$ ), pitchfork (at  $(x, \alpha) = (0, 6)$ ) and transcritical (at  $(x, \alpha) = (0, -30)$ ) bifurcations. Using affine linear transformations of  $x$  and  $\alpha$ , we reorient Eq. 1 around each bifurcation point. We construct training and test data by simulating for various parameter values; 10 such test traces clubbed together are presented for each bifurcation scenario (in blue) in Fig. 3.

Results are presented in Fig. 3. We show learned test data (blue) and normal form simulations (gray), together for 10 traces. These traces correspond to different initial values and parameters. The simulations are performed by using the learned parameter and initial condition from the learned time traces. We observe agreement across different cases, for all bifurcation scenarios. We note that the parameter orientation loss was not used ( $\lambda_5 = 0$ ) in the transcritical case, to allow the parameters (blue) to orient themselves properly with respect to the normal form ( $\alpha \mapsto -\alpha$ ). In the remaining two bifurcations, the learned (blue) and original (orange) parameters have the same sign. Moreover,

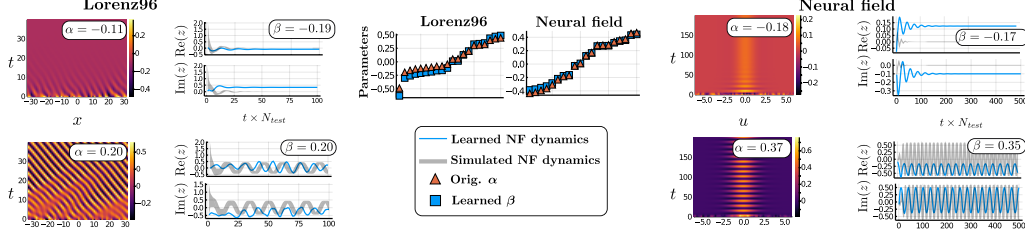


Figure 4: Results for the two high-dimensional systems, Eq.2 and Eq. 3. In both cases, training and test data contain 1000 and 20 traces, respectively.  $\Phi_1$  has widths [32, 16] (Lorenz96) and [64, 32, 16] (Neural field).  $\varphi_1$  has widths [16, 16] in both cases.

in the case of pitchfork and transcritical bifurcations, the zero loss ensures that the trivial equilibrium  $x = 0$  is preserved.

**Hopf bifurcation in the Lorenz96 system.** The Lorenz96 equations [27] are used widely in model discovery and data assimilation problems. The equations are given by

$$\dot{x}_j = -x_{j-1}(x_{j-2} - x_{j+1}) - x_j + \alpha \quad (2)$$

for  $j = 1, 2, 3 \dots N$  with boundary conditions  $x_1 = x_N$  and  $x_2 = x_{N-1}$ . In this work we set  $N = 64$ . For this choice of  $N$ , the trivial equilibrium  $x = \alpha$  undergoes a supercritical Hopf bifurcation with respect to  $\alpha$  at  $\alpha = \alpha_0 = 0.84975$  [28]. Using affine linear transformations of  $x$  and  $\alpha$ , we first reorient Eq. 2 around  $(x, \alpha) = (\alpha_0, \alpha_0)$  such that the bifurcation now occurs at  $(x, \alpha) = (0, 0)$ . Simulations of the system before and after the bifurcation point are shown in Fig. 4. For  $\alpha < 0$ , we observe the existence of a stable stationary solution, while for  $\alpha > 0$  we observe a spatiotemporal stripe pattern, which is interpreted as a travelling wave.

Results are presented in Fig. 4. For two choices of  $\alpha$  on different sides of the bifurcation point, we plot learned (blue) and simulated time traces from test data, that match well qualitatively. The high dimensional periodic pattern is encoded to a stable periodic solution, and the stationary solution is encoded into a damped oscillation. The encoding of the time traces match well with parameter encoding, as the sign of the original parameters (orange) is the same as the learned parameters (blue).

**Hopf bifurcation in a neural field equation.** Next, we consider a neural field equation describing the neuronal potential for a one-dimensional continuum of neural tissue [29, 30]. The spatiotemporal dynamics due to an input inhomogeneity lead to a Hopf bifurcation of a stationary pattern leading to breathers when varying the input strength [31, 32]. The equations are given by,

$$\begin{aligned} \dot{u} &= -u - \kappa a + (w * f(u)) + I(x), \\ \dot{a} &= (-a + u)/\tau_{nf}. \end{aligned} \quad (3)$$

The operator  $*$  represents a spatial convolution.  $w(x) \equiv w(x - y) = w_e \exp(-((x - y)/\sigma_e)^2)$  is the spatial connectivity kernel and  $f(u)$  is the potential-dependent sigmoidal firing rate given by  $f(u) = (1 + \exp(\beta_{nf}(u - u_{thr})))^{-1}$ . The spatially non-uniform input  $I(x)$  is given by  $I(x) = \alpha \exp(-(x/\sigma)^2)$ .

We fix  $\kappa = 2.75$ ,  $\tau_{nf} = 10$ ,  $w_e = 1$ ,  $\sigma_e = 1$ ,  $\beta_{nf} = 6$ ,  $u_{thr} = 0.375$ ,  $\sigma = 1.2$ . The parameter  $\alpha$  is used as the bifurcation parameter. A supercritical Hopf bifurcation with respect to a stationary bump response occurs at  $\alpha = 0.8040$ . States  $u, a$  are discretized over a uniform grid of size 64 each. Like before, we first reorient Eq. 3 such that the bifurcation occurs at  $(u, a, \alpha) = (0, 0, 0)$ . Setting  $\alpha < 0$  produces the globally asymptotically stable stationary bump response. This is shown for the variable  $u$  in Fig. 4. For  $\alpha > 0$ , we see that the stationary bump loses stability and the emerging asymptotically stable periodic solution expands and contracts, referred to as ‘breathers’ [32].

Results are presented in Fig. 4. Similar to the Lorenz96 case, we present learned test data for two cases,  $\alpha < 0$  and  $\alpha > 0$ . Once again, the qualitative behaviour of the time-traces match the Hopf normal form dynamics and are supported by the parameter encodings. The sign of the learned parameters are the same as the original parameters. In both Lorenz96 and the neural field equations, fixing the orientation loss helps avoid local minima and other symmetry-induced feasible solutions by fixing the sign of the learned parameters and thus, the direction of the bifurcation.

## Conclusion

We have demonstrated a deep learning approach to uncover a coordinate transformation into a single, parameterized normal form equation that describes the parametric dependence of a data set over a range of values. Our approach has consequences for dynamical systems theory and data-driven model discovery alike. The approach can be extended to discover underlying low-dimensional models by using normal forms as building blocks. On the other hand, this presents a novel method to compute center manifold restrictions, which is an important problem in applied dynamical systems theory.

## References

- [1] John Guckenheimer and Philip Holmes. *Nonlinear Oscillations, Dynamical Systems, and Bifurcations of Vector Fields*. Springer New York, 1983.
- [2] P. J. Holmes, J. L. Lumley, G. Berkooz, and C. W. Rowley. *Turbulence, coherent structures, dynamical systems and symmetry*. Cambridge Monographs in Mechanics. Cambridge University Press, Cambridge, England, 2nd edition, 2012.
- [3] Gal Berkooz, Philip Holmes, and John L Lumley. The proper orthogonal decomposition in the analysis of turbulent flows. *Annual review of fluid mechanics*, 25(1):539–575, 1993.
- [4] K. Willcox and J. Peraire. Balanced model reduction via the proper orthogonal decomposition. *AIAA Journal*, 40(11):2323–2330, 2002.
- [5] Clarence W Rowley. Model reduction for fluids, using balanced proper orthogonal decomposition. *International Journal of Bifurcation and Chaos*, 15(03):997–1013, 2005.
- [6] Peter J Schmid. Dynamic mode decomposition of numerical and experimental data. *Journal of fluid mechanics*, 656:5–28, 2010.
- [7] Jonathan H. Tu, Clarence W. Rowley, Dirk M. Luchtenburg, Steven L. Brunton, and J. Nathan Kutz. On dynamic mode decomposition: Theory and applications. *Journal of Computational Dynamics*, 1(2158-2491-2014-2-391):391, 2014.
- [8] Qianxiao Li, Felix Dietrich, Erik M. Bollt, and Ioannis G. Kevrekidis. Extended dynamic mode decomposition with dictionary learning: A data-driven adaptive spectral decomposition of the koopman operator. *Chaos: An Interdisciplinary Journal of Nonlinear Science*, 27(10):103111, 2017.
- [9] Kunihiko Taira, Steven L Brunton, Scott Dawson, Clarence W Rowley, Tim Colonius, Beverley J McKeon, Oliver T Schmidt, Stanislav Gordeyev, Vassilios Theofilis, and Lawrence S Ukeiley. Modal analysis of fluid flows: An overview. *AIAA Journal*, 55(12):4013–4041, 2017.
- [10] Steven L Brunton, Joshua L Proctor, and J Nathan Kutz. Discovering governing equations from data by sparse identification of nonlinear dynamical systems. *Proceedings of the national academy of sciences*, 113(15):3932–3937, 2016.
- [11] Samuel H. Rudy, Steven L. Brunton, Joshua L. Proctor, and J. Nathan Kutz. Data-driven discovery of partial differential equations. *Science Advances*, 3(4):e1602614, apr 2017.
- [12] Naoya Takeishi, Yoshinobu Kawahara, and Takehisa Yairi. Learning koopman invariant subspaces for dynamic mode decomposition. In *Advances in Neural Information Processing Systems*, pages 1130–1140, 2017.
- [13] Enoch Yeung, Soumya Kundu, and Nathan Hodas. Learning deep neural network representations for koopman operators of nonlinear dynamical systems. *arXiv preprint arXiv:1708.06850*, 2017.
- [14] Christoph Wehmeyer and Frank Noé. Time-lagged autoencoders: Deep learning of slow collective variables for molecular kinetics. *The Journal of Chemical Physics*, 148(241703):1–9, 2018.
- [15] Andreas Mardt, Luca Pasquali, Hao Wu, and Frank Noé. VAMPnets: Deep learning of molecular kinetics. *Nature Communications*, 9(5), 2018.
- [16] Bethany Lusch, J. Nathan Kutz, and Steven L. Brunton. Deep learning for universal linear embeddings of nonlinear dynamics. *Nature Communications*, 9(1):4950, dec 2018.
- [17] Pantelis R Vlachas, Wonmin Byeon, Zhong Y Wan, Themistoklis P Sapsis, and Petros Koumoutsakos. Data-driven forecasting of high-dimensional chaotic systems with long short-term memory networks. *Proc. R. Soc. A*, 474(2213):20170844, 2018.

- [18] Jaideep Pathak, Brian Hunt, Michelle Girvan, Zhixin Lu, and Edward Ott. Model-free prediction of large spatiotemporally chaotic systems from data: a reservoir computing approach. *Physical review letters*, 120(2):024102, 2018.
- [19] Kathleen Champion, Bethany Lusch, J. Nathan Kutz, and Steven L. Brunton. Data-driven discovery of coordinates and governing equations. *Proceedings of the National Academy of Sciences*, 116(45):22445–22451, nov 2019.
- [20] Samuel E. Otto and Clarence W. Rowley. Linearly recurrent autoencoder networks for learning dynamics. *SIAM Journal on Applied Dynamical Systems*, 18(1):558–593, 2019.
- [21] Francesco Regazzoni, Luca Dedè, and Alfio Quarteroni. Machine learning for fast and reliable solution of time-dependent differential equations. *Journal of Computational Physics*, 397:108852, 2019.
- [22] Yohai Bar-Sinai, Stephan Hoyer, Jason Hickey, and Michael P Brenner. Learning data-driven discretizations for partial differential equations. *Proceedings of the National Academy of Sciences*, 116(31):15344–15349, 2019.
- [23] Alec J Linot and Michael D Graham. Deep learning to discover and predict dynamics on an inertial manifold. *Physical Review E*, 101(6):062209, 2020.
- [24] Maziar Raissi, Alireza Yazdani, and George Em Karniadakis. Hidden fluid mechanics: Learning velocity and pressure fields from flow visualizations. *Science*, 367(6481):1026–1030, 2020.
- [25] Kookjin Lee and Kevin T Carlberg. Model reduction of dynamical systems on nonlinear manifolds using deep convolutional autoencoders. *Journal of Computational Physics*, 404:108973, 2020.
- [26] Yu. A. Kuznetsov. *Elements of Applied Bifurcation Theory*, volume 112 of *Applied Mathematical Sciences*. Springer-Verlag, New York, third edition, 2004.
- [27] Edward N. Lorenz. *Predictability – a problem partly solved*, page 40–58. Cambridge University Press, 2006.
- [28] Dirk L. van Kekem and Alef E. Sterk. Travelling waves and their bifurcations in the lorenz-96 model. *Physica D: Nonlinear Phenomena*, 367:38 – 60, 2018.
- [29] Shun-ichi Amari. Dynamics of pattern formation in lateral-inhibition type neural fields. *Biological cybernetics*, 27(2):77–87, 1977.
- [30] Hugh R Wilson and Jack D Cowan. Excitatory and inhibitory interactions in localized populations of model neurons. *Biophysical journal*, 12(1):1–24, 1972.
- [31] Stefanos E. Folias. Nonlinear analysis of breathing pulses in a synaptically coupled neural network. *SIAM Journal on Applied Dynamical Systems*, 10(2):744–787, 2011.
- [32] S. Coombes and M. R. Owen. Bumps, breathers, and waves in a neural network with spike frequency adaptation. *Phys. Rev. Lett.*, 94:148102, Apr 2005.